Acta Geophysica (2026) 74:37
https://doi.org/10.1007/s11600-025-01755-7

RESEARCH ARTICLE - ATMOSPHERIC & SPACE SCIENCES

Earth's electric field in Greece during the 2024 Mother's Day or Gannon geomagnetic superstorm

Efthimios S. Skordas[1] · **Nicholas V. Sarlis**[1] · **Panayiotis A. Varotsos**[1]

Received: 8 July 2025 / Accepted: 24 November 2025

Abstract
On 10 May 2024, a geomagnetic superstorm causing the largest geomagnetic disturbance since 2003 started because of the shock arrival at Earth from multiple coronal mass ejections at 17:05UT. In Greece, the magnetic disturbance was recorded by the Pedeli (PEG) magnetic observatory of the INTERMAGNET global network of observatories. At the same time, VAN telemetric network, installed in the 1980 s and 1990 s for earthquake prediction purposes, measured the electric field of the Earth at several field stations in Greece. Here, we report these measurements during this Mother's Day or Gannon geomagnetic superstorm that lasted from 10 to 12 May 2024. We also show how the geoelectric data can be combined with the geomagnetic variations for an estimation of the resistivity at different locations in Greece. The present results are useful for the estimation of geomagnetically induced currents which constitute a major hazard for electric power networks.

Keywords Electric field of the Earth · Geomagnetic storms · Resistivity · VAN telemetric network

Introduction

Geomagnetic storms are worldwide disturbances of the Earth's magnetic field due to the terrestrial ring current, an electric current flowing in a toroidal pattern in near-Earth space (Daglis et al. 1999). Intensified ring current results from enhanced solar wind–magnetosphere interaction (Gonzalez et al. 1994). When the rapidly changing geomagnetic field interacts with the solid Earth can create geomagnetically induced currents (GICs) the intensity of which depends on the distribution of the electrical properties in specific areas of the Earth's solid crust (Daglis et al. 2003; Balasis et al. 2006; Boteler 2003). Most GICs are triggered by coronal mass ejections (CMEs), which interact with the magnetic field around the Earth and cause it to rattle. The quick-changing magnetic fields create GICs through electromagnetic induction. GICs are the ground end of the space weather chain, e.g., Sun solar wind–magnetosphere–ionosphere–Earth's surface. GIC occurrence poses a hazard that can potentially cause damage by quasi-DC currents that can arise in long conductors, such as power transmission lines or oil pipelines (Pulkkinen et al. 2001, 2005; Daglis et al. 2001). The auroral oval occasionally extends down to reach the geomagnetic latitudes of Greece (see Knipp, Delores J. et al. 2021; Hayakawa et al. 2021, 2023,) and may potentially cause GIC effects to such a lower geomagnetic latitude too.

On 10 May 2024 at 17:05UT a powerful impact arrived (Hayakawa et al. 2025; Piersanti et al. 2025; Astafyeva et al. 2025) at Earth originating from multiple CMEs from the active region 3664 of the Sun (Liu et al. 2024; Tulasi Ram et al. 2024; Hayakawa et al. 2025). This gave rise to a geomagnetic superstorm that lasted over 40 h (Gonzalez-Esparza et al. 2024) while another CME arrived at 22:20UT, being the strongest storm over a period of more than 20 years, since the Halloween 2003 superstorm (see, e.g., Yamazaki et al. (2024); Hayakawa et al. (2025)). Astafyeva et al. (2025) studied the SYM-H index (Iyemori 1990; Iyemori et al. 2010) (see also Wanliss and Showalter

Edited by Dr. Oleksiy Dudnik (ASSOCIATE EDITOR) / Prof. Theodore Karacostas (CO-EDITOR-INCHIEF).

✉ Efthimios S. Skordas
eskordas@phys.uoa.gr

Nicholas V. Sarlis
nsarlis@phys.uoa.gr

Panayiotis A. Varotsos
pvaro@otenet.gr

[1] Department of Physics, Section of Condensed Matter Physics and Solid Earth Physics Institute, National and Kapodistrian University of Athens, Panepistimiopolis, 157 84 Athens, Greece

Published online: 21 December 2025

(2006)) and found that it showed an excursion with minimum -497nT (5-min data) setting this geomagnetic storm the largest since March 1989, for SYM-H (1min) see the lowest panel of Fig. 1. This geomagnetic superstorm was named Mother's Day geomagnetic storm (see, e.g., Spogli et al. 2024; Gonzalez-Esparza et al. 2024; Wang et al. 2025,) or Gannon Storm (see, e.g., Schennetten et al. 2024; Clilverd et al. 2025,) in honor of the late Dr Jennifer Gannon (Lugaz et al. 2024). The related GICs have been studied by Clilverd et al. (2025) in New Zealand and by Piersanti et al. (2025) in Europe, while apparent resistivity observation networks in China have been severely impacted (Zhang et al. 2025).

In our study, we focus on the effects of this geomagnetic superstorm in Greece and make use of the International Real-Time Magnetic Observatory Network INTERMAGNET (see, e.g. INTERMAGNET; et al. 2021,) that provides freely the data from various magnetic observatories around the world at https://imag-data.bgs.ac.uk/GIN_V1/GINForms2. The uppermost panel of Fig. 1 depicts the geomagnetic field components and the total magnetic field measured at Pedeli (PEG) geomagnetic station located at N38.1^{o}E23.9^o (close to Athens, Greece) with elevation h =380 m while in the middle panel we include for completeness (since there are some missing data at PEG) the corresponding measurements at Panagjurishte (PAG) geomagnetic station located in Bulgaria at N42.515^{o}E24.177^o with elevation h =556 m. Inspection of Fig. 1 reveals the impact of the aforementioned arrivals of the CMEs at 17.05UT and 22:20UT on the geomagnetic field in southern Balkan peninsula. We observe a sharp increase of the X component of the geomagnetic field at around 17.05UT and a sharp peak at 22:20UT of the total field at PEG. Similarly, at PAG the X & Y components as well as the total field exhibit sudden changes at 17:05 and 22:20UT on 10 May 2024.

We now turn to the geoelectric measurements during this superstorm. These have been acquired by means of the VAN telemetric network (Varotsos 2005; Varotsos et al. 2011) (see Fig. 2). This comprises a network of field stations in which the electric field of the Earth is measured by a multitude of measuring electric dipoles (see, e.g., Varotsos and Lazaridou (1991); Varotsos et al. (1993)) aiming at the detection of seismic electric signals (SES) which are low-frequency ($\leq$ 1Hz) variations of the electric (Sarlis and Varotsos 2002,) and magnetic field of the Earth that precede earthquakes (EQs) (Varotsos and Alexopoulos 1984; Varotsos and Lazaridou 1991; Varotsos et al. 1993; Uyeda et al. 2000, 2002; Sarlis et al. 2008; Uyeda and Kamogawa 2008; Uyeda et al. 2009; Ramírez-Rojas et al. 2011; Sarlis 2013; Orihara et al. 2012; Sarlis and Skordas 2018; Ramírez-Rojas et al. 2018). In early 1980 s, the Greek scientists Varotsos, Alexopoulos, and Nomicos (Varotsos et al. 1981a, b) found that continuous measurements of the electric field of the Earth reveals EQ precursory signals and for this reason the acronym VAN is used worldwide (Uyeda 1996; Lazaridou-Varotsos 2013; Sarlis et al. 2018). Data are collected and transmitted in real time(Nomicos and Chatzidiakos 1993; Nomicos et al. 1996; Varotsos 2005) to the central station at Glyfada which is a suburb of Athens (ATH), see Fig. 2. Additionally dataloggers (Campbell 21X) are also installed to collect data with sampling rate f_s =1 sample/sec and the data are transmitted 5 times per day to ATH via internet (see, e.g., Skordas et al. 2025). It is the latter geoelectric data of the VAN stations Assiros (ASS), Ioannina (IOA), Volos (VOL), Patras (PAT), Loutraki (LOU), and Pirgos (PIR), which are shown in Fig. 2 during the Mother's Day or Gannon geomagnetic superstorm that will be analyzed in the present paper.

The data used and the method of analysis will be presented in the next Section 2. The results will appear in Section 3 and will be discussed in Section 4. Finally, our conclusions will be presented in Section 5.

Data and methods

Data

Geomagnetic data

All geomagnetic data come from INTERMAGNET (see, e.g., INTERMAGNET; et al. 2021,) and are freely available from https://intermagnet.org/, as mentioned in Introduction. Data with sampling rate f_s = 1sample/min are shown in Fig. 1 for the PEG and PAG stations (for their locations see the map in Fig. 2). Here, we also make use of the f_s = 1 sample/sec data from PEG, which are available by INTERMAGNET (see Fig. 3) and focus on the onset of the geomagnetic superstorm. The analysis of these data together with the geolectric measurements (see Section 2.1.2) provides useful information on the resistivity at the sites of the measuring dipoles.

Geoelectric data

As mentioned in Introduction, geoelectric data come from the six stations (ASS, IOA, VOL, PAT, LOU, PIR) of the VAN telemetric network (Varotsos 2005; Varotsos et al. 2011) shown in Fig. 2. Non-polarizable electrodes $Pb/PbCl_2$ at a depth of 2 m are used and the potential difference ΔV between pairs of electrodes separated at a distance L is measured. In the region around each VAN station, short and long measuring electric dipoles of lengths L varying from a few tens of m to several km are deployed with various true bearings φ according to the criteria suggested by Varotsos and Lazaridou (1991); Varotsos et al. (1993) for

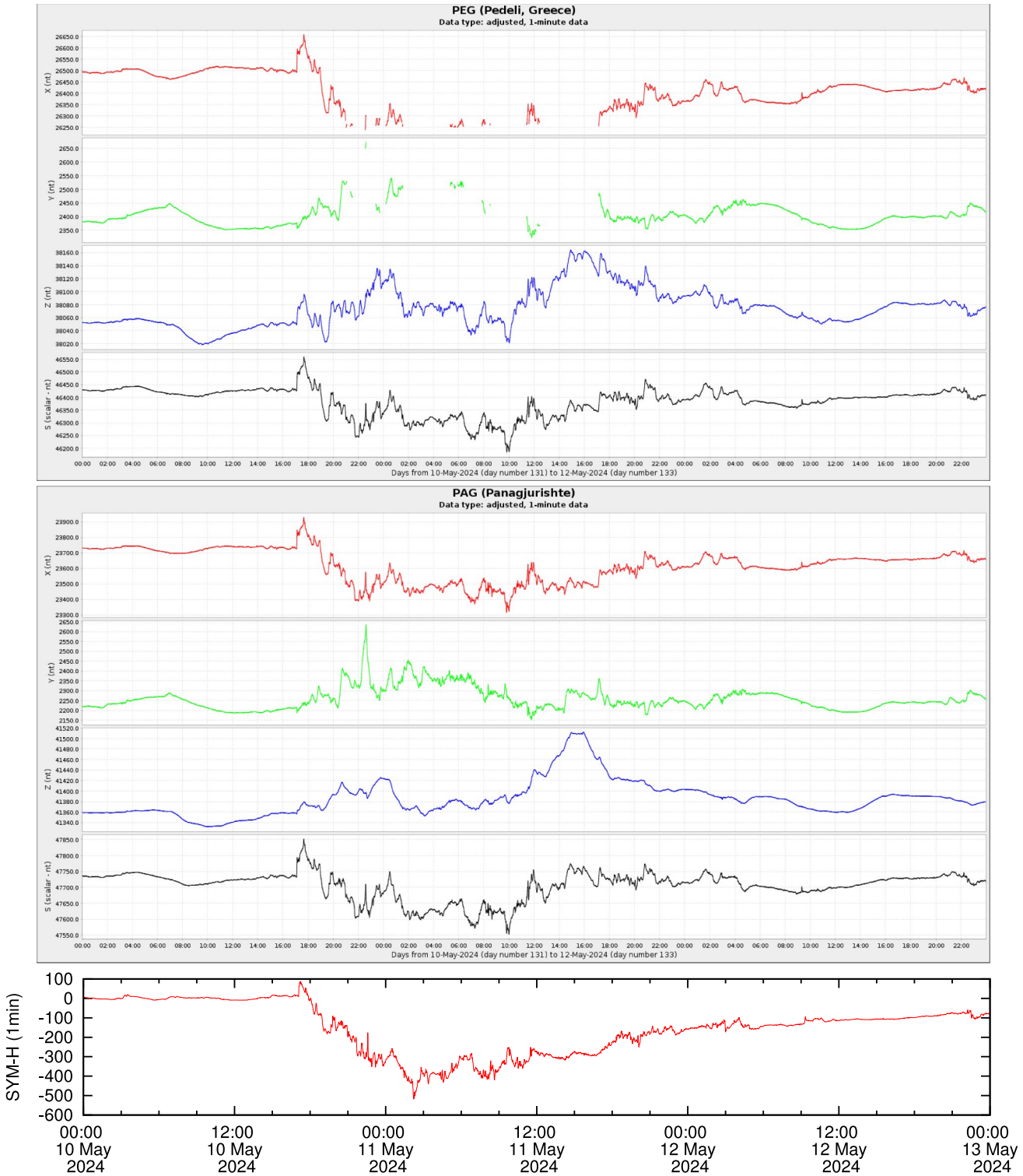

Fig. 1 The X (North), Y(East), Z(down) components and the total S magnetic field in nT recorded by PEG and PAG geomagnetic stations of the INTERMAGNET network (INTERMAGNET; et al. 2021) during 10 May 2024 00:00UT to 13 May 2024 00:00UT, i.e., during the Mother's Day or Gannon geomagnetic superstorm. In the lowest panel, we depict SYM-H (Imajo et al. 2022) which is calculated every 1min from data of 6 magnetic observatories distributed in longitude and latitude (see also Iyemori 1990,). SYM-H is freely available from https://isgi.unistra.fr

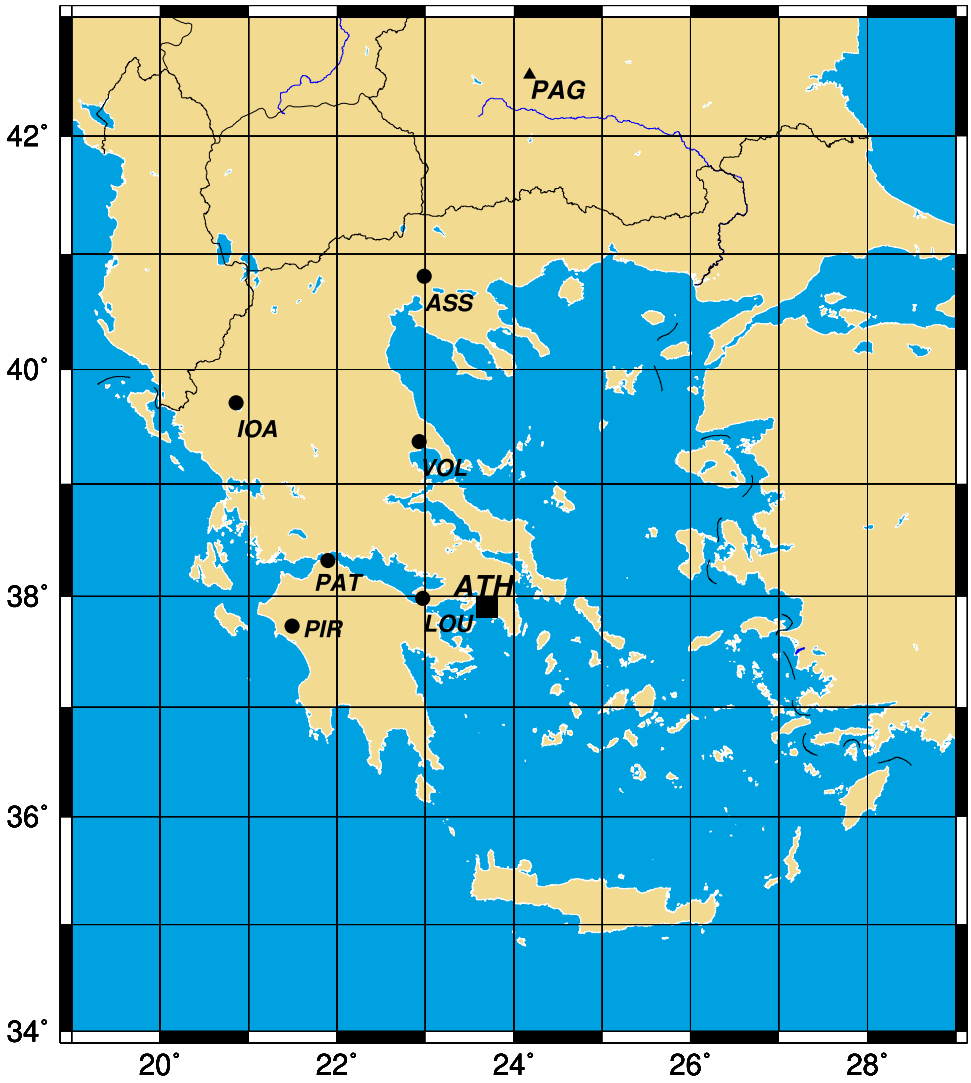

Fig. 2 Map of Greece where the geolectric stations Assiros (ASS), Ioannina (IOA), Volos (VOL), Patras (PAT), Loutraki (LOU), and Pirgos (PIR) are depicted with full circles. The geolectric data are transmitted real-time to the Athens (ATH) central station of the VAN telemetric network(Varotsos 2005; Varotsos et al. 2011). The location of the geomagnetic station at PAG in Bulgaria is also shown with a triangle, cf. the location of the PEG station (which is close to Athens) in Greece overlaps with ATH

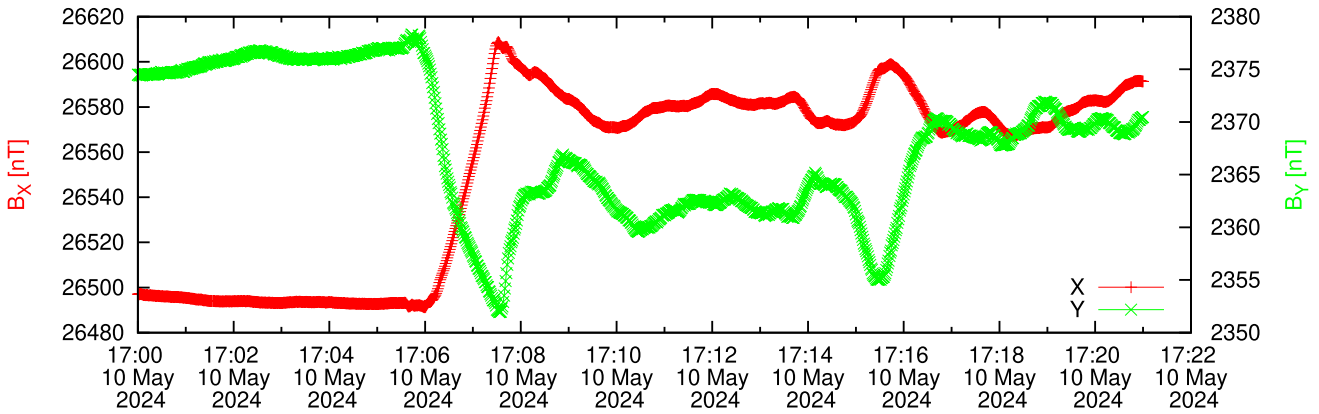

Fig. 3 The horizontal components of the magnetic field at PEG with sampling rate f_s =1sample/sec upon the arrival of the first three merged CMEs of the geomagnetic superstorm

the discrimination of SES from other signals originated from human activity and civilization (see also Skordas et al. 2010).

Interrelation of the electric and the magnetic field of the earth in the case of a condutive half-space

Assuming that during the geomagnetic storm the electromagnetic field arriving at the surface of the Earth is a transverse plane wave propagating downwards and approximating the Earth as a conductive half-space of resistivity ρ_H, Pirjola (1989) estimates the time domain electric field component $E_y(t)$ by the relationship (see also Pirjola 1982; Wait 1954; Cagniard 1953,):

$$E_y(t) = -\sqrt{\frac{\rho_H}{\pi\mu_0}}\int_0^\infty \frac{g_x(t-u)}{\sqrt{u}}du, \tag{1}$$

where $g_x(t) \equiv \frac{d\mathrm{B_X}}{dt}$ is the time derivative of the North magnetic field component $\mathrm{B_X}(t)$ and μ_0 the magnetic permeability of vacuum. An equation similar to Eq. (1) relates $E_x(t)$ with $g_y(t) \equiv \frac{d\mathrm{B_Y}}{dt}$ the time derivative of the East magnetic field component $\mathrm{B_Y}(t)$. The assumption of more complicated conductivity structures for the Earth leads to more complicated expressions, see, e.g., Pirjola (1982).

The above means that we can firstly differentiate and then appropriately integrate the horizontal components of the magnetic field measured at PEG (shown in Fig. 3) to obtain the quantities

$$\mathrm{E_Y}(t) = \int_0^\infty \frac{d\mathrm{B_X}}{dt}(t-u)\frac{du}{\sqrt{u}} \tag{2}$$

and

$$\mathrm{E_X}(t) = \int_0^\infty \frac{d\mathrm{B_Y}}{dt}(t-u)\frac{du}{\sqrt{u}} \tag{3}$$

which are proportional to the instantaneous values of $E_y(t)$ and $E_x(t)$, respectively, having units of $\mathrm{nT}\sqrt{\mathrm{Hz}}$ as can be seen from Eq. (1). Figure 4 shows how the potential difference $\Delta V(t)$ of a measuring dipole can then be related to either $\mathrm{E_Y}(t)$:

$$\Delta V(t) = -\sqrt{\frac{\rho_H}{\pi\mu_0}}L\sin(\varphi)\mathrm{E_Y}(t) \tag{4}$$

or $\mathrm{E_X}(t)$:

$$\Delta V(t) = \sqrt{\frac{\rho_H}{\pi\mu_0}}L\cos(\varphi)\mathrm{E_X}(t). \tag{5}$$

By observing the behavior of the time evolution of $\Delta V(t)$, we can select which of the two Eqs. (4) or (5) should be used to estimate ρ_H from our geolectric field recordings. This is the subject of the next Section 3.

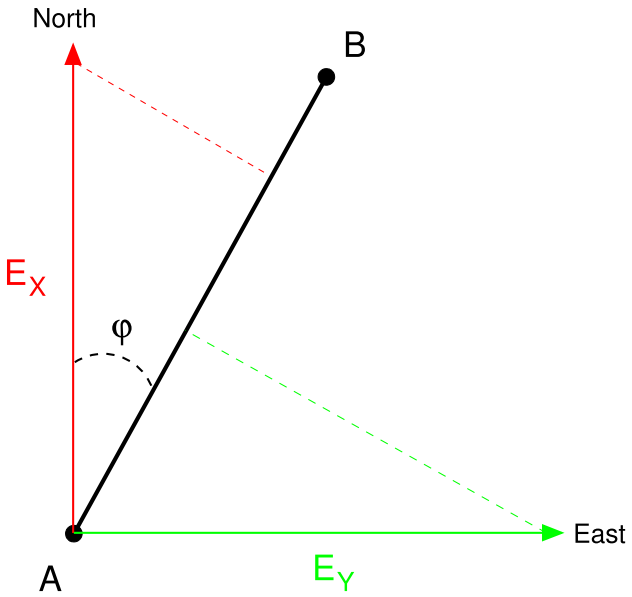

Fig. 4 The measuring dipole AB records the projection of the geolectric field on its bearing

Results

Figures 5 and 6 show the potential difference ΔV with $f_s = 1$ sample/sec between electrodes of various measuring dipoles, called for brevity channels (CH), versus the conventional time during the period 10 May 2024 00:00UT to 13 May 2024 00:00UT. Each channel is characterized by its length L and its true bearing φ; more details for each VAN station can be found in Varotsos (2005).

Estimation of resistivity

We now turn to the estimation of the resistivity on the basis of the geoelectric measurements shown in Figs. 5 and 6 in conjuction with the magnetic field measurements of $f_s = 1$ sample/sec at PEG (see Fig. 3), during the onset of the geomagnetic superstorm. Inspection of Figs. 5 and 6 reveals that many channels behave similarly with the components of the horizontal magnetic field at PEG during the arrival of the geomagnetic superstorm. To investigate this further, we numerically calculate $\mathrm{E_Y}(t)$ and $\mathrm{E_X}(t)$ using Eqs. (2) and (3), respectively, and compare the results with those recorded by the measuring dipoles of the VAN telemetric network.

Figure 7 shows typical examples of two measuring dipoles from each VAN station that show a time evolution similar to that of either $\mathrm{E_Y}(t)$ or $\mathrm{E_X}(t)$. The detailed characteristics of each channel shown in Fig. 7 are reported in

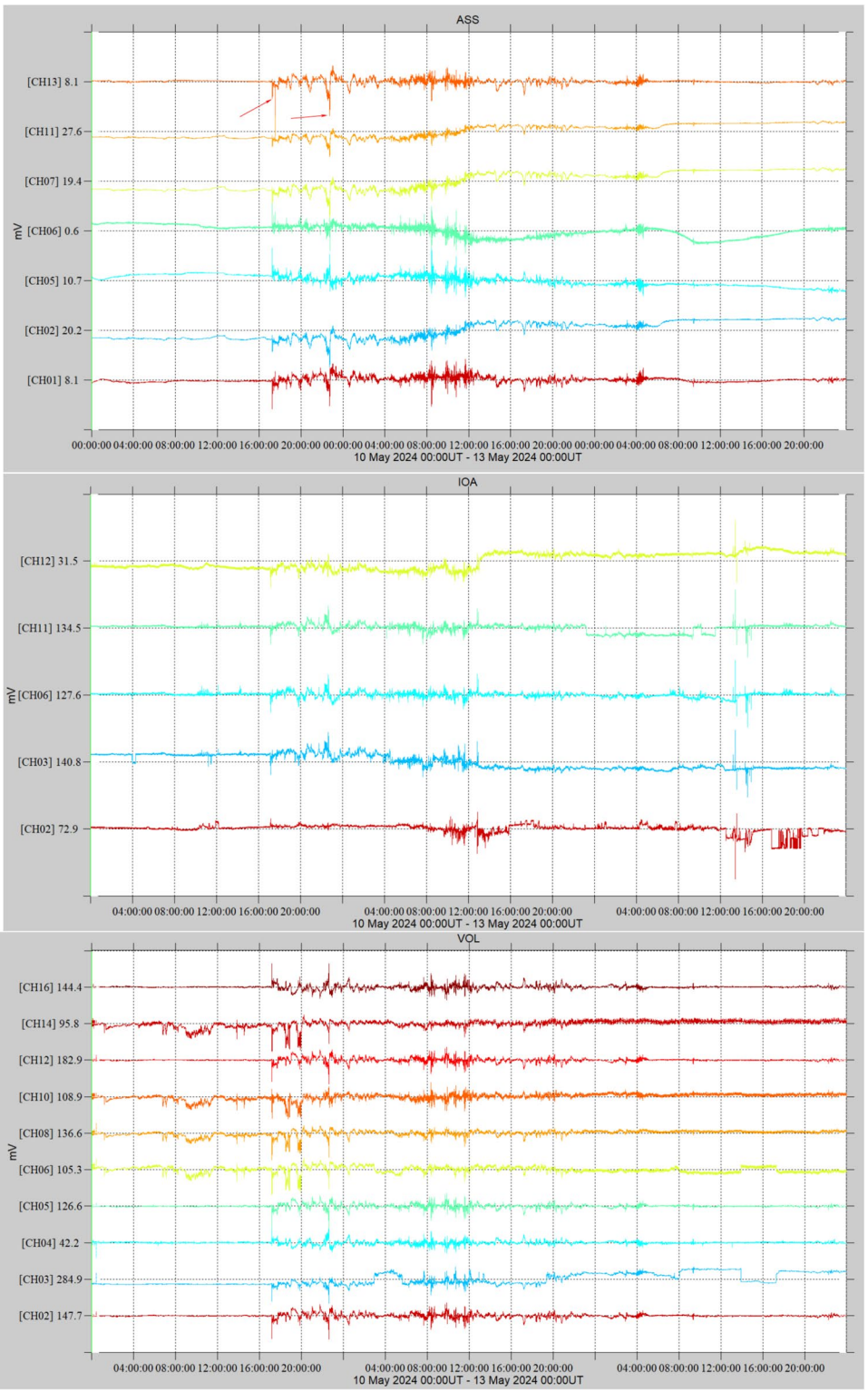

Fig. 5 Recordings of the potential difference ΔV between the electrodes of the measuring dipoles (channels, CH) for ASS, IOA and VOL geoelectric VAN stations. The name of the geolectric station is written in the title of each panel. The horizontal ticks are evenly distributed every 4 h (the time stamp 00:00UT may not be written for reasons of clarity), while the numbers at each vertical tick correspond to 1/10 of the range in mV between consecutive vertical ticks for the channel whose ΔV starts close to the tick. The two red arrows in the uppermost panel indicate the geoelectric field variations associated with the arrival of the CMEs at 17:05UT and 22:20UT on 10 May 2024

Table 1 and can be used for the estimation of ρ_H. This can be done as follows: When we observe that the time evolution of a channel follows the time evolution of either $E_X(t)$ or $E_Y(t)$, take, for example, CH01 and CH02 of PIR station (see Fig. 7C and D), we plot $\Delta V(t)$ versus $E_X(t)$ or $E_Y(t)$ in the form of a polarization diagram (see, e.g., Makris et al. 1999; Makris 2001). Such a diagram is shown in Fig. 8, and we observe a clear linear correlation which is due to Eqs. (4) and (5). The linear least squares fit shown (thick

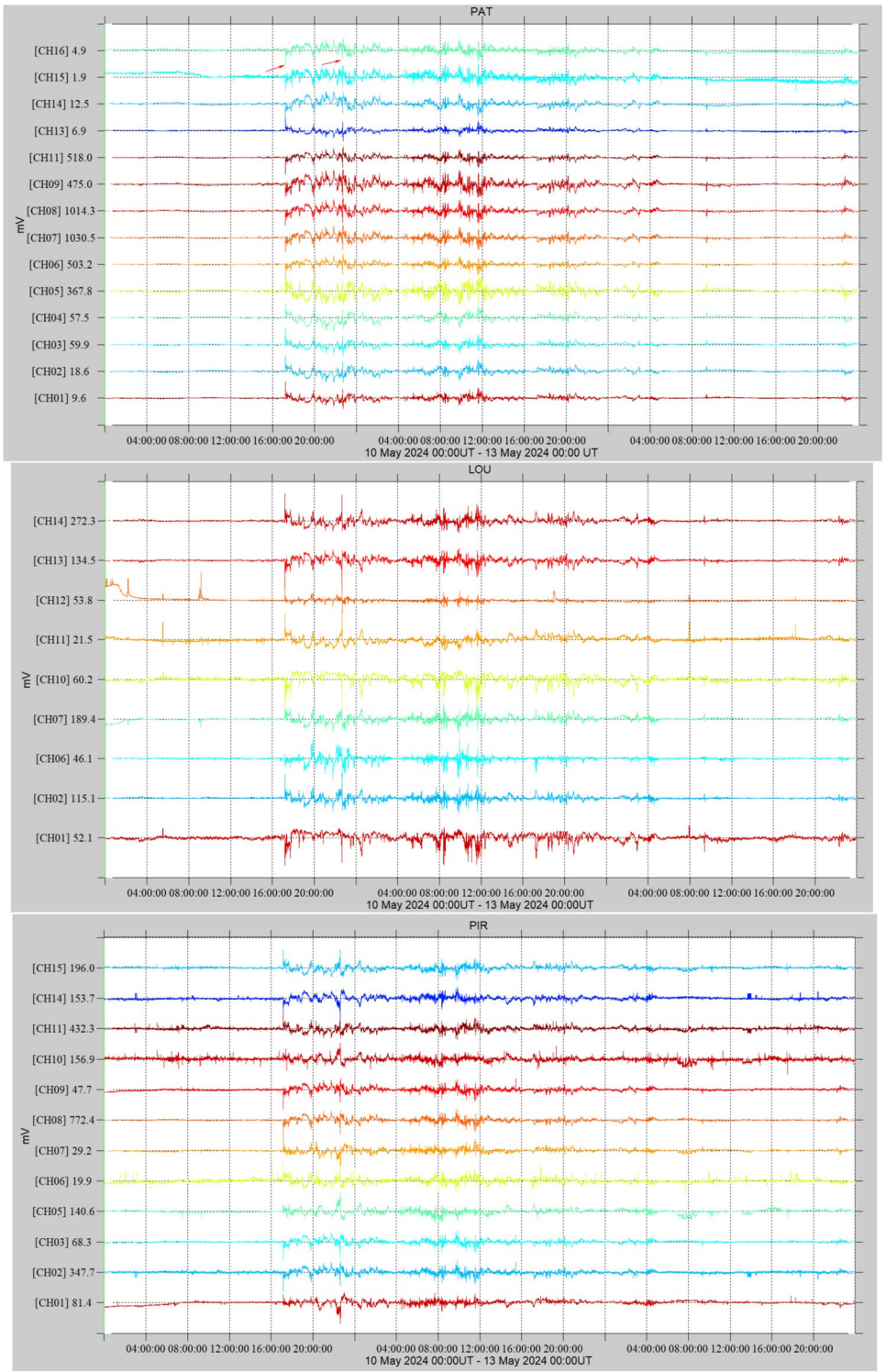

Fig. 6 The same as Fig. 5 but for the geoelectric stations PAT, LOU, and PIR. The numbers at each vertical tick correspond to 1/10 of the range in mV between consecutive vertical ticks for the channel whose ΔV starts close to the tick. The two red arrows in the uppermost panel indicate the geoelectric field variations related to the arrival of the CMEs at 17:05UT and 22:20UT on 10 May 2024

green lines) allows the estimation of the slope $\sqrt{\frac{\rho_H}{\pi\mu_0}}L \times [\sin(\varphi) \text{ or } \cos(\varphi)]$ in Eqs. (4) and (5), and therefrom, we can estimate ρ_H and its plausible error.

Figure 9 shows the values of ρ_H estimated by using various channels in each VAN station as a function of either the longitude (A) or the latitude (B) of the station. In Fig. 9B, we observe a systematic behavior shown by the green line that will be discussed in the next Section 4.

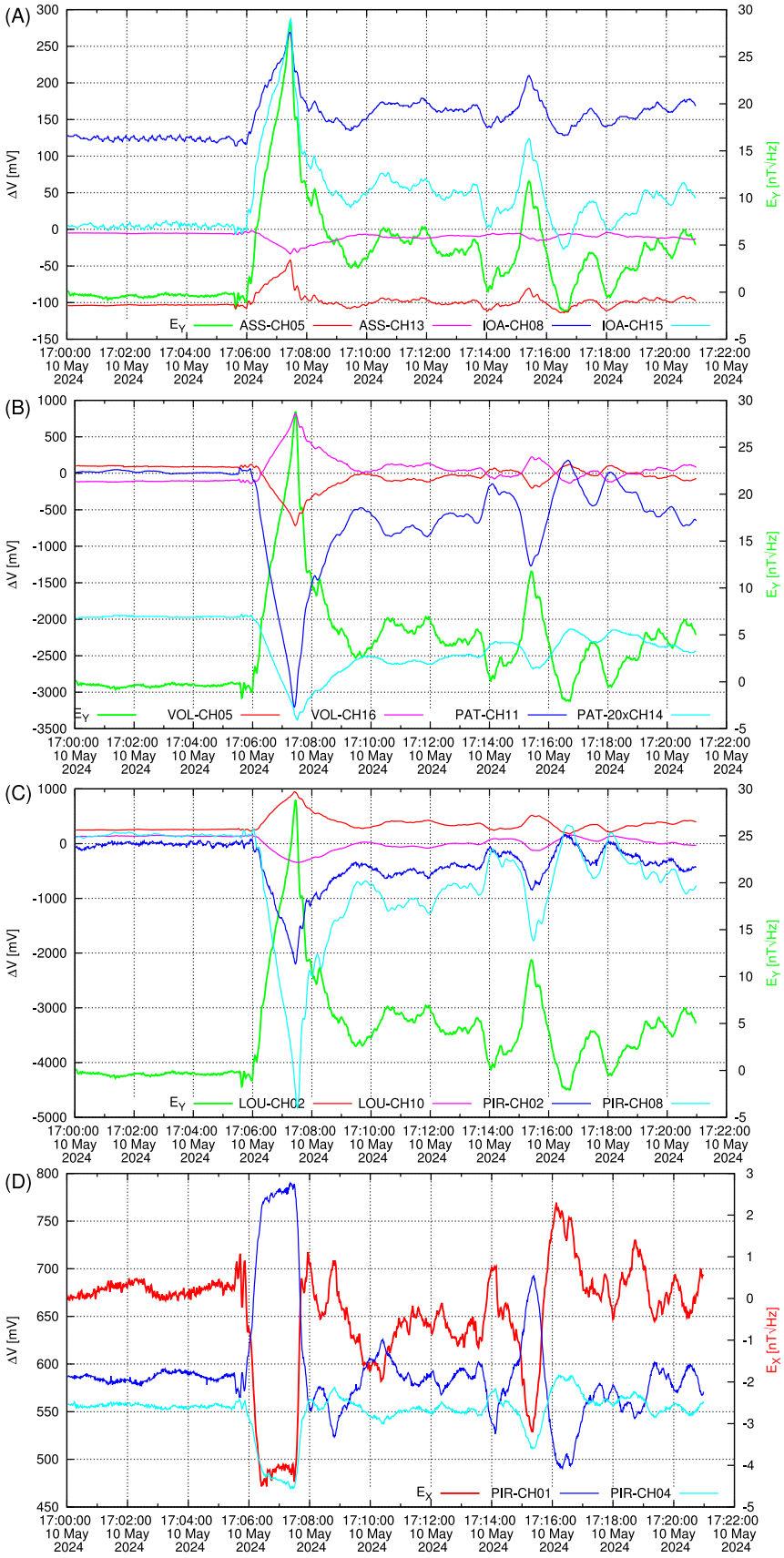

Fig. 7 Recordings of the potential difference $\Delta V(t)$ between the electrodes of measuring dipoles from the geoelectric stations ASS, IOA, VOL, PAT, LOU, and PIR. In each panel, we also depict either $E_Y(t)$ or $E_X(t)$, to be read on the right scale, depending on which of the two resembles the time evolution of the geoelectric field

Table 1 The length L and true bearing φ of the channels shown in Fig. 7. In the last column, the values of ρ_H calculated according to the method described in Section 3.1 are inserted

VAN station	CH	L [km]	φ [^{o}T]	ρ_H [Ω m]
ASS	5	0.069	91.0	(115 ± 5)
ASS	13	0.277	324.5	(160 ± 30)
IOA	8	0.110	123.6	(510 ± 30)
IOA	15	0.053	88.4	(229 ± 14)
VOL	5	1.930	90.0	(970 ± 160)
VOL	16	2.259	285.0	(980 ± 130)
PAT	11	4.233	95.0	(2970 ± 260)
PAT	14	0.149	305.0	(1500 ± 700)
LOU	2	12.466	26.0	(104 ± 21)
LOU	10	13.277	18.6	(85 ± 30)
PIR	1	3.522	10.0	(24 ± 3)
PIR	2	4.670	102.0	(11.7 ± 0.6)
PIR	4	1.172	16.0	(33 ± 4)[1]
PIR	8	11.106	86.0	(9.9 ± 0.7)

[1]These values come from E_X

Discussion

The VAN telemetric network, as mentioned, records the potential difference ΔV between pairs of electrodes separated at a distance L. These data can give information on the ground electric field (GEF) produced by the geomagnetic storm at various sites in Greece. A critical parameter in GIC modeling is the GEF which is rarely measured directly (Marshalko et al. 2023).

Figures 5 and 6 report these measurements at a sampling rate of f_s=1sample/sec during Mother's day or Gannon geomagnetic superstorm. The potential difference ΔV exhibits characteristic variations from 10 May 2024 17:05 UT until around 12 May 2024 05:30UT. The electric disturbances due to this geomagnetic superstorm arrive at all stations of the VAN telemetric network shown in Fig. 2 almost at the same time with a clear onset. This onset can be seen in an expanded time scale in Fig. 7 (A), (B), and (C) for selected channels that correspond to the electric field component E_y while examples of channels resembling the electric field component E_x are shown in Fig. 7(D).

There are two periods where the recorded electric field is more intense, i.e., from 10 May 2024 17:05UT until 11 May 2024 02:00UT and from 11 May 2024 04:00UT until 11 May 2024 13:00 UT. During the first period, we have the arrival at 17:05UT of the three merged CMEs as well as the arrival of another CME at 20:20UT which are clearly discernable as sudden changes of the geoeletric field, see the red arrows in Figs. 5 and 6. The "sudden" increase of ΔV at 17:05UT on 10 May 2024 can be better visualized in Fig. 7 where it is revealed that it lasts about 90sec, in accordance with the geomagnetic field variations of Fig. 3 at PEG. Secondary geomagnetic field variations like the one at 17:15UT are also well reflected in the geoelectric field, see, e.g., Fig. 7. The second period of intense ΔV, i.e., from 04:00UT to 13:00UT on 11 May 2024, occurs after the minimization of SYM-H at 02:15UT on 11 May 2024 during the recovering phase probably due to the fact that SYM-H varies frequently until 12:00UT on 11 May 2024 (see the lowest panel of Fig. 1). It should be noted, however, that SYM-H does not coincide with the maxima of GEF which are largely influenced by the time derivative of the geomagnetic field, see Eq. (1).

We now turn to the opportunity of measuring ρ_H using the geoelectromagnetic field at the onset of the geomagnetic superstorm. If the situation is such that the potential difference ΔV recorded at a channel of the VAN network

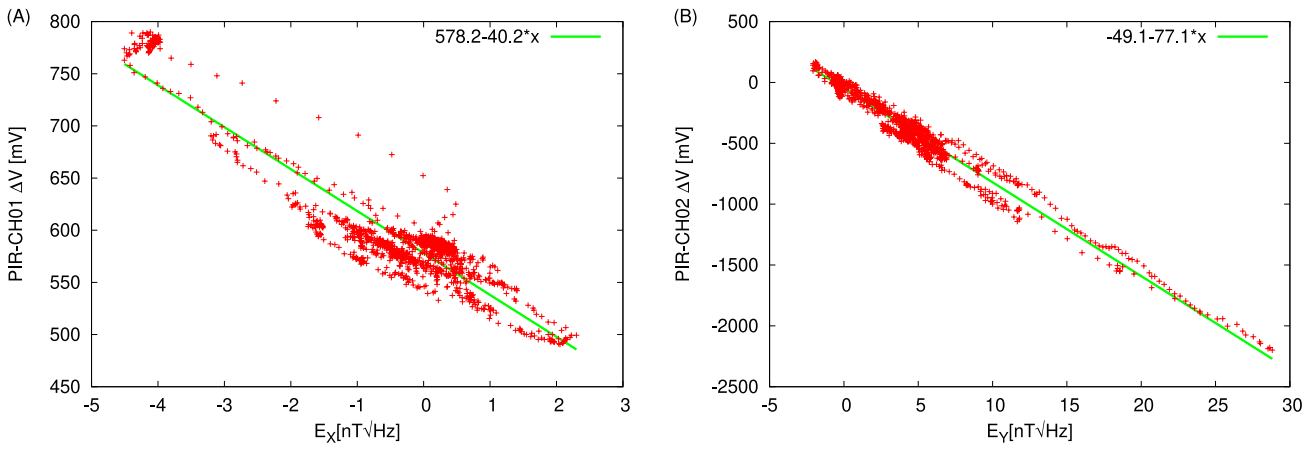

Fig. 8 The recording $\Delta V(t)$ versus $E_X(t)$ (A) or $E_Y(t)$ (B) for the channels CH01 and CH02 of PIR, respectively. The thick green line corresponds to a least squares fit of the data shown in Fig. 7(C) and (D)

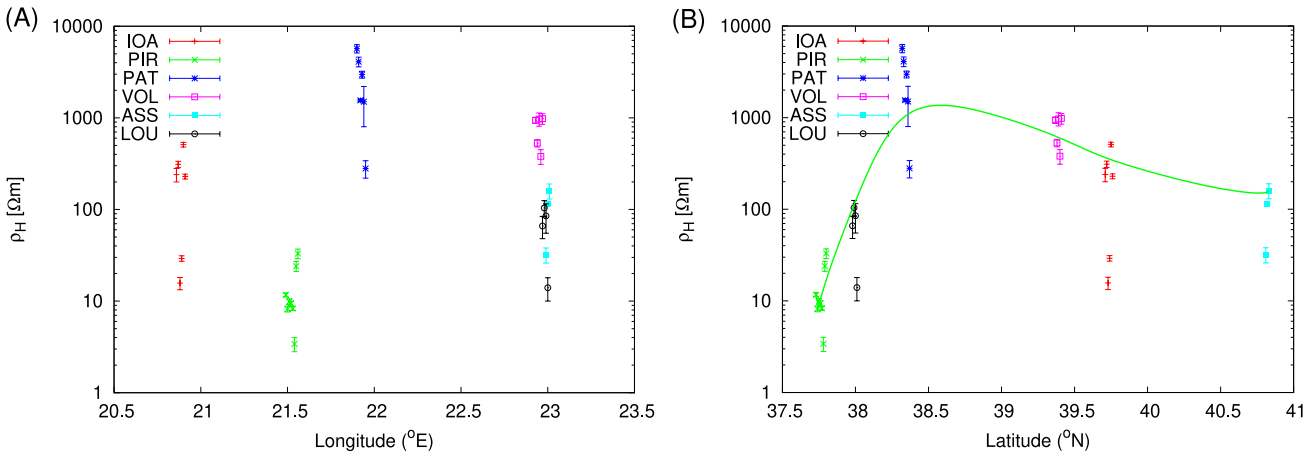

Fig. 9 The resistivities ρ_H found for measuring electric dipoles deployed at the various VAN stations with the method of Section 3.1 versus (A) the longitude and (B) the latitude. Channels within the same station are shifted to the right by 0.01^o to avoid overlap. The green curve in (B) has been drawn as a guide to the eye

closely follows the one predicted for a conductive half-space of resistivity ρ_H then a simple least square fit, like the one shown in Fig. 8, can lead to an estimation of ρ_H. The application of this method to all channels of the VAN network that satisfy the aforementioned prerequisite leads to the resistivities reported in Fig. 9. There, we observe that although across longitude no certain features can be seen, when we study ρ_H vs. latitude and travel from South to the North we first see a sharp increase and then a gradual decrease from 1000 s to 100 s of Ωm. This is certainly a feature that should be taken into account when calculating GICs in Greece; for a recent study, see Boutsi et al. (2023); see also Boutsi et al. (2025).

Conclusions

We studied the potential differences ΔV measured by the VAN network in Greece during the Mother's Day or Gannon geomagnetic superstorm. We found that there are two periods at which large values of ΔV are observed. These are upon the arrival of the CMEs at 17:05 and 22:20UT on 10 May 2024 while the second period is after the minimization of SYM-H.

During the first period at the onset of the geomagnetic superstorm, the behavior of ΔV in a large number of measuring electric dipoles follows closely the time evolution expected from a conductive half-space of resistivity ρ_H. By numerically integrating the horizontal magnetic field measured at PEG station of the INTERMAGNET network, we are able to calculate ρ_H.

The values of ρ_H obtained show a clear behavior versus latitude that could be used for estimating GICs in Greece.

We hope that in the future the ΔV data of the VAN network operating in Greece since 1980 s will be further used for the mitigation of the hazard imposed by geomagnetic superstoms in Greece.

Acknowledgements We gratefully acknowledge the continuous supervision and technical support of the geoelectrical stations of the VAN telemetric network by Vasilis Dimitropoulos, Spyros Tzigkos and George Lampithianakis.

Author Contributions **Efthimios S. Skordas** contributed to conceptualization, methodology, formal analysis, investigation, writing—original draft preparation, writing—reviewing and editing, supervision, project administration. **Nicholas V. Sarlis** contributed to conceptualization, methodology, software, formal analysis, investigation, resources, writing—original draft preparation, writing—reviewing and editing, visualization. **Panayiotis A. Varotsos** contributed to conceptualization, methodology, software, formal analysis, investigation, resources, data curation, writing—original draft preparation, writing—reviewing and editing, visualization.

Funding The authors did not receive support from any organization for the submitted work.

Data availability The data that support the findings of this study are available from the corresponding author upon reasonable request.

Code availability The codes used in this study are available from the corresponding author upon reasonable request.

Declarations

Conflict of interest The authors declare that they have no known competing financial interests or personal relationships that could have appeared to influence the work reported in this paper.

Ethics approval N/A

Consent to participate N/A

Consent for publication N/A

References

Astafyeva E, Maletckii B, Förster M et al (2025) Electrodynamic and ionospheric puzzles of the 10 11 May 2024 geomagnetic superstorm. J Geophys Res: Space Phys 130(5):e2024JA033284. https://doi.org/10.1029/2024JA033284

Balasis G, Daglis IA, Kapiris P et al (2006) From pre-storm activity to magnetic storms: a transition described in terms of fractal dynamics. Ann Geophys 24(12):3557–3567. https://doi.org/10.5194/angeo-24-3557-2006

Boteler DH (2003) Geomagnetic hazards to conducting networks. Nat Hazards 28:537–561. https://doi.org/10.1023/A:1022902713136

Boutsi AZ, Balasis G, Dimitrakoudis S et al (2023) Investigation of the geomagnetically induced current index levels in the mediterranean region during the strongest magnetic storms of solar cycle 24. Space Weather 21(2):e2022SW003122. https://doi.org/10.1029/2022SW003122

Boutsi AZ, Papadimitriou C, Balasis G et al (2025) Dynamical complexity in geomagnetically induced current activity indices using block entropy. Entropy 27(2):172. https://doi.org/10.3390/e27020172

Cagniard L (1953) Basic theory of the magnetotelluric method of geophysical prospecting. Geophysics 18(3):605–635. https://doi.org/10.1190/1.1437915

Clilverd MA, Rodger CJ, Manus DHM et al (2025) Geomagnetically induced currents, transformer harmonics, and reactive power impacts of the gannon storm in May 2024. Space Weather 23(4):e2024SW004235. https://doi.org/10.1029/2024SW004235

Daglis IA, Thorne RM, Baumjohann W et al (1999) The terrestrial ring current: Origin, formation, and decay. Rev Geophys 37(4):407–438. https://doi.org/10.1029/1999RG900009

Daglis IA, Baker DN, Galperin Y et al (2001) Technological impacts of space storms: outstanding issues. EOS Trans Am Geophys Union 82(48):585–592. https://doi.org/10.1029/01EO00340

Daglis IA, Kozyra JU, Kamide Y, et al (2003) Intense space storms: critical issues and open disputes. J Geophys Res: Space Phys108(A5). https://doi.org/10.1029/2002JA009722

Gonzalez WD, Joselyn JA, Kamide Y et al (1994) What is a geomagnetic storm? J Geophys Res Space Phys 99(A4):5771–5792. https://doi.org/10.1029/93JA02867

Gonzalez-Esparza JA, Sanchez-Garcia E, Sergeeva M et al (2024) The mother's day geomagnetic storm on 10 May 2024: Aurora observations and low latitude space weather effects in Mexico. Space Weather 22(11):e2024SW004111. https://doi.org/10.1029/2024SW004111

Hayakawa H, Hattori K, Pevtsov AA et al (2021) The intensity and evolution of the extreme solar and geomagnetic storms in 1938 January. Astrophys J 909(2):197. https://doi.org/10.3847/1538-4357/abc427

Hayakawa H, Cliver EW, Clette F et al (2023) The extreme space weather event of 1872 February: Sunspots, magnetic disturbance, and auroral displays. Astrophys J 959(1):23. https://doi.org/10.3847/1538-4357/acc6cc

Hayakawa H, Ebihara Y, Mishev A et al (2025) The solar and geomagnetic storms in 2024 May: A flash data report. Astrophys J 979(1):49. https://doi.org/10.3847/1538-4357/ad9335

Imajo S, Matsuoka A, Toh H, et al. (2022) Mid-latitude Geomagnetic Indices ASY and SYM (ASY/SYM Indices). https://doi.org/10.14989/267216 World Data Center for Geomagnetism, Kyoto

INTERMAGNET; et al (2021) Intermagnet reference data set (IRDS) 2018 definitive magnetic observatory data. GFZ Data Services., https://doi.org/10.5880/INTERMAGNET.1991.2018

Iyemori T (1990) Storm-time magnetospheric currents inferred from mid-latitude geomagnetic field variations. J Geomagn Geoelectr 42(11):1249–1265. https://doi.org/10.5636/jgg.42.1249

Iyemori T, Takeda M, Nose M, et al (2010) Mid-latitude geomagnetic indices ASY and SYM for 2009 (Provisional), Kyoto University, Japan, pp I–X

Knipp DJ, Bernstein V, Wahl K et al (2021) Timelines as a tool for learning about space weather storms. J Space Weather Space Clim 11:29. https://doi.org/10.1051/swsc/2021011

Lazaridou-Varotsos MS (2013) Earthquake Prediction by Seismic Electric Signals. Springer-Verlag, Berlin Heidelberg, The success of the VAN method over thirty years. https://doi.org/10.1007/978-3-642-24406-3

Liu YD, Hu H, Zhao X et al (2024) A pileup of coronal mass ejections produced the largest geomagnetic storm in two decades. Astrophys J Lett 974(1):L8. https://doi.org/10.3847/2041-8213/ad7ba4

Lugaz N, Knipp D, Morley SK et al (2024) In memoriam of editor Jennifer L Gannon. Space Weather 22(6):e2024SW004016. https://doi.org/10.1029/2024SW004016

Makris J (2001) Properties of the geoelectric structure that promote the detection of electrotelluric anomalies: The case of Ioannina Greece. Annals Geophys 44(2):313–324. https://doi.org/10.4401/ag-3598

Makris J, Bogris N, Eftaxias K (1999) A new approach in the determination of characteristic directions of the geoelectric structure using Mohr circles. Earth, Planets and Space 51(10):1059–1065. https://doi.org/10.1186/BF03351579

Marshalko E, Kruglyakov M, Kuvshinov A et al (2023) Three-dimensional modeling of the ground electric field in fennoscandia during the Halloween geomagnetic storm. Space Weather 21(9):e2022SW003370. https://doi.org/10.1029/2022SW003370

Nomicos K, Chatzidiakos P (1993) A telemetric system for measuring electrotelluric variations in Greece and its application to earthquake prediction. Tectonophysics 224(1):39–46. https://doi.org/10.1016/0040-1951(93)90056-P

Nomicos K, Makris J, Kefalas M (1996) The telemetric system of VAN group, in the critical review of VAN: earthquake prediction from seismic electric signals. In: J.Lighthill S (ed) The Critical Review of VAN: Earthquake Prediction from Seismic Electric Signals. World Scientific, Singapore, pp 77–88, https://doi.org/10.1142/3006

Orihara Y, Kamogawa M, Nagao T et al (2012) Preseismic anomalous telluric current signals observed in Kozu-shima Island, Japan. Proc Natl Acad Sci USA 109(47):19125–19128. https://doi.org/10.1073/pnas.1215669109

Piersanti M, Oliveira DM, D'Angelo G et al (2025) On the geoelectric field response to the SSC of the May 2024 super storm over Europe. Space Weather 23(2):e2024SW004191. https://doi.org/10.1029/2024SW004191

Pirjola R (1982) Electromagnetic induction in the Earth by a plane wave or by fields of line currents harmonic in time and space. Geophysica 18:1–161

Pirjola R (1989) Geomagnetically induced currents in the Finnish 400 kV power transmission system. Phys Earth Planet Inter 53(3):214–220. https://doi.org/10.1016/0031-9201(89)90005-8

Pulkkinen A, Viljanen A, Pajunp K et al (2001) Recordings and occurrence of geomagnetically induced currents in the Finnish natural gas pipeline network. J Appl Geophys 48(4):219–231. https://doi.org/10.1016/S0926-9851(01)00108-2

Pulkkinen A, Lindahl S, Viljanen A et al (2005) Geomagnetic storm of 29-31 October 2003: Geomagnetically induced currents and their relation to problems in the Swedish high-voltage power transmission system. Space Weather 3(8):S08C03. https://doi.org/10.1029/2004SW000123

Ramírez-Rojas A, Telesca L, Angulo-Brown F (2011) Entropy of geoelectrical time series in the natural time domain. Nat Hazards Earth Syst Sci 11:219–225. https://doi.org/10.5194/nhess-11-219-2011

Ramírez-Rojas A, Flores-Márquez EL, Sarlis NV et al (2018) The complexity measures associated with the fluctuations of the entropy

in natural time before the deadly Mexico M.82 Earthquake on 7 September 2017. Entropy 20(6):477. https://doi.org/10.3390/e20060477

Sarlis N, Varotsos P (2002) Magnetic field near the outcrop of an almost horizontal conductive sheet. J Geodyn 33:463–476. https://doi.org/10.1016/S0264-3707(02)00008-X

Sarlis NV (2013) On the recent seismic activity in North-Eastern Aegean Sea including the M_{w} 5.8 earthquake on 8 January 2013. Proc Jpn Acad Ser B Phys Biol Sci 89:438–445. https://doi.org/10.2183/pjab.89.438

Sarlis NV, Skordas ES (2018) Study in natural time of geoelectric field and seismicity changes preceding the Mw6.8 Earthquake on 25 October 2018 in Greece. Entropy 20:882. https://doi.org/10.3390/e20110882

Sarlis NV, Skordas ES, Lazaridou MS et al (2008) Investigation of seismicity after the initiation of a seismic electric signal activity until the main shock. Proc Jpn Acad Ser B Phys Biol Sci 84:331–343. https://doi.org/10.2183/pjab.84.331

Sarlis NV, Varotsos PA, Skordas ES et al (2018) Seismic electric signals in seismic prone areas. Earthquake Sci 31:44–51. https://doi.org/10.29382/eqs-2018-0005-5

Schennetten K, Matthi D, Meier MM et al (2024) The impact of the Gannon Storm of May 2024 on the radiation fields at aviation altitudes and in low earth orbits. Front Astron Space Sci 11:1498910. https://doi.org/10.3389/fspas.2024.1498910

Skordas ES, Sarlis NV, Varotsos PA (2010) Effect of significant data loss on identifying electric signals that precede rupture estimated by detrended fluctuation analysis in natural time. Chaos 20:033111. https://doi.org/10.1063/1.3479402

Skordas ES, Sarlis NV, Varotsos PA (2025) Possible detection of the onset of flash flooding in Thessaly Greece by measurements of the Earth s surface electric field. Nat Hazards 121:8613–8629. https://doi.org/10.1007/s11069-025-07145-y

Spogli L, Alberti T, Bagiacchi P et al (2024) The effects of the May 2024 Mother's Day superstorm over the Mediterranean sector: from data to public communication. Annals Geophys 67(2):PA218. https://doi.org/10.4401/ag-9117

Tulasi Ram S, Veenadhari B, Dimri AP et al (2024) Super-intense geomagnetic storm on 10 11 May 2024: possible mechanisms and impacts. Space Weather 22(12):e2024SW004126. https://doi.org/10.1029/2024SW004126

Uyeda S (1996) Introduction to the VAN method of earthquake prediction. In: Lighthill SJ (ed) The Critical Review of VAN: Earthquake Prediction from Seismic Electric Signals, vol 16. World Scientific, Singapore, pp 3–28. https://doi.org/10.1142/3006

Uyeda S, Kamogawa M (2008) The prediction of two large Earthquakes in Greece. Eos Trans AGU 89:363. https://doi.org/10.1029/2008EO390002

Uyeda S, Nagao T, Orihara Y et al (2000) Geoelectric potential changes: Possible precursors to earthquakes in Japan. Proc Natl Acad Sci USA 97:4561–4566. https://doi.org/10.1073/pnas.97.9.4561

Uyeda S, Hayakawa M, Nagao T et al (2002) Electric and magnetic phenomena observed before the volcano-seismic activity in 2000 in the Izu Island Region, Japan. Proc Natl Acad Sci USA 99:7352–7355. https://doi.org/10.1073/pnas.072208499

Uyeda S, Kamogawa M, Tanaka H (2009) Analysis of electrical activity and seismicity in the natural time domain for the volcanic-seismic swarm activity in 2000 in the Izu Island region. Japan J Geophys Res 114:B02310. https://doi.org/10.1029/2007JB005332

Varotsos P (2005) The Physics of Seismic Electric Signals. TERRAPUB, Tokyo

Varotsos P, Alexopoulos K (1984) Physical Properties of the variations of the electric field of the Earth preceding earthquakes, I. Tectonophysics 110:73–98. https://doi.org/10.1016/0040-1951(84)90059-3

Varotsos P, Lazaridou M (1991) Latest aspects of earthquake prediction in Greece based on seismic electric signals. Tectonophysics 188:321–347. https://doi.org/10.1016/0040-1951(91)90462-2

Varotsos P, Alexopoulos K, Nomicos K (1981a) Seismic electric currents. Practica Athens Acad 56:277–286

Varotsos P, Alexopoulos K, Nomicos K (1981b) Seven-hour precursors to earthqaukes determined from telluric currents. Practica Athens Acad 56:417–433

Varotsos P, Alexopoulos K, Lazaridou M (1993) Latest aspects of earthquake prediction in Greece based on Seismic Electric Signals, II. Tectonophysics 224:1–37. https://doi.org/10.1016/0040-1951(93)90055-O

Varotsos PA, Sarlis NV, Skordas ES (2011) Natural Time Analysis: The new view of time. Springer-Verlag, Berlin Heidelberg, Precursory Seismic Electric Signals, Earthquakes and other Complex Time-Series. https://doi.org/10.1007/978-3-642-16449-1

Wait JR (1954) On the relation between telluric currents and the earths magnetic field. Geophysics 19(2):281–289. https://doi.org/10.1190/1.1437994

Wang X, Aa E, Chen Y et al (2025) Midlatitude neutral wind response during the Mother's Day super-intense geomagnetic storm in 2024 using observations from the Chinese meridian project. J Geophys Res: Space Phys 130(4):e2024JA033574. https://doi.org/10.1029/2024JA033574

Wanliss JA, Showalter KM (2006) High-resolution global storm index: Dst versus SYM-H. J Geophys Res (Space Physics) 111(A2):A02202. https://doi.org/10.1029/2005JA011034

Yamazaki Y, Matzka J, Silva MVSd, et al (2024) Assessment of Kp=9 geomagnetic storms including the May 2024 Gannon storm based on version 3.0 Hpo indices. Earth and Space Science Open Archive https://doi.org/10.22541/essoar.171838396.68563140/v2

Zhang X, Xie T, Ye Q et al (2025) Severe distortion of the apparent resistivity induced by the super geomagnetic storm in May 2024. Geophys Res Lett 52(8):e2025GL115104. https://doi.org/10.1029/2025GL115104